



# High-standard farmland destruction monitoring by high-resolution remote sensing methods: a 2017–2018 case study of Hebei and Guangdong, China

Admire Muchimamui Mutelo · Chen Zhen · Shen Wei · Shindume Lomboleni Hamukwaya

Received: 7 January 2023 / Accepted: 4 May 2023 / Published online: 26 May 2023  
© The Author(s), under exclusive licence to Springer Nature Switzerland AG 2023

**Abstract** Remote sensing has emerged as a new technique for collecting farmland data due to its rapid advancement, rising popularity, and application in social production practice. In order to understand and manage farmland resources in China, it is essential to account for and monitor high-standard farmland and its usage. Therefore, this work used satellite remote sensing empowered with various abilities for monitoring high-standard farmland by employing GF-2 high-resolution satellite images to identify targets and objects in Hebei and Guangdong provinces. Farmland occupation and utilization were analyzed by detecting destructions, underutilization, and overutilization, and converting farmland for other economic activities registered on a special field sheet for quantification. A statistical summary was compiled for the two provinces, and the results reveal that high-standard

farmland irregularities were detected in both Hebei and Guangdong provinces. However, in Hebei province, this was due to domestic purposes, such as building home shelters and domestic factories. On a contract, the result shows that in Guangdong province, farmland was being converted for economic purposes on an industrial scale, such as high residential apartment blocks and new industrial zones, and environmental destruction. Furthermore, the results reveal that there is still a steady and continuous decline in arable land due to accelerated industrialization and population pressure, especially in the Guangdong provinces, which is a threat to national food security. The high interpretation accuracy demonstrates that high-resolution remote sensing is an effective farmland monitoring tool that can be used to advance policy formulation.

---

A. M. Mutelo (✉) · C. Zhen (✉) · S. Wei  
School of Earth Sciences and Resources, China University of Geosciences, 29 Xueyuan Road, BeijingBeijing 100083, China  
e-mail: admiremutelo@yahoo.com

C. Zhen  
e-mail: chenzhen@cugb.edu.cn

S. Wei  
e-mail: shenwei@cugb.edu.cn

S. L. Hamukwaya  
School of Science, China University of Geosciences, Beijing 100083, China  
e-mail: shamukwaya@unam.na

**Keywords** Remote sensing · Land monitoring · Land use · Land cover · Farm land

## Introduction

Remote sensing (RS) of the earth has come a long way which can be traced back to nineteenth-century aerial photography to the latest high-resolution satellite and unmanned aerial vehicle (UAV) remote sensing. Though it began in the military, at present remote sensing means satellite observations, and it began in 1972 with the launch of Landsat-1 for civilian applications

(Roy et al., 2017). In recent times, the satellite remote sensing field has seen an increase in innovative novel advances such as new higher spatial resolution optical and radar systems, hyperspectral sensors, important by-products such as digital elevation model (DEM), and additionally the development of new processing techniques by application of machine learning (Roy et al., 2017). Remote sensing by UAV (RS UAV) has emerged due to the development of robotics, computer vision, and sensor miniaturization (Alvarez-Vanhard et al., 2021). High-standard farmland is characterized by better-equipped facilities than basic farmland and is featured by reasonable layout and network of land, irrigation canals, roads, and concentrated and flat, well-equipped, high-yield, and ecologically sound farmland (Hu et al., 2010).

Plans to construct more than 5.33 million ha of high-standard farmland in 2018 arose from the 13th session of the National People's Congress (Luoman et al., 2019). In 2011, China established its first specification for high-quality agricultural land development. Since then, academics in the country have used a wide range of tools to evaluate these projects' efficacy and determine how best to evaluate the construction's content. Researchers compiled a list of the materials used to build high-quality farmland and evaluated its quality. Others have utilized GIS and spatial analysis to evaluate the efficacy of farmland improvement projects by tracking changes in crop yields and farmer incomes (Luoman et al., 2019).

RS is applied as a monitoring tool among various specializations, and it has been used in environmental monitoring, such as landfill sites and mining (Yan et al., 2014). In addition to the in situ observation network, satellite remote sensing is being increasingly used to provide information on crop yield and irrigation at multiple spatial and temporal scales, independent of geopolitical boundaries (Karthikeyan et al., 2020).

In addition, various methods are used for environmental monitoring in various settings, such as the following: evaluation of land use and land cover change due to desertification, land reclamation, soil sealing, or urban sprawl; evaluation of water quality in both inland and open waters; mapping of surface lithology (Bitelli et al., 2017).

In comparison to older technologies, remote sensing has numerous advantages. Remote sensing allows for continuous geographical and temporal monitoring and mapping, unlike discrete frequency point

measurements. Thus, RS data and methodologies can improve environmental decision-making in settings where environmental modifications and impacts are regularly observed (Ghauri & Zaidi, 2011).

Spectral signatures are key elements, each object has a unique spectral signature that identifies it, and spectral properties are re-observed by the reflectance curve.

In a country of more than a billion people, a decline in arable land and high demand for food push farmers to produce more to meet the rising demand. On the other hand, continuous steady industrialization has caused tremendous spatial concerns for the authorities. The government seeks to protect arable land from exploitation through high-standard farmland construction.

By 2030, China will have 80 million hectares of high-quality farmland; this is significant because farmland is the basis for food security and plays a critical role in the ecosystem and green agricultural development. There are plans to upgrade more farmland through the proposed guideline by upgrading up to 280 million units (mu) of high-standard farmland by 2030. China continues to develop basic farmland into high-standard farmland to increase productivity, leading to a sustainable food supply for its population.

Because of the country's progress in creating high-quality farmland measured in mu, it boosted its grain-producing capacity by 10–20% per mu while simultaneously reducing its per-mu cost to the tune of 77.7 US dollars (Luoman et al., 2019).

However, as China has become increasingly industrialized in recent years, there is a greater possibility that farmland will be converted into other income-generating projects. The rising demand for agricultural goods may lead some farmers to disregard the stringent farmland construction guidelines imposed by the Ministry of Lands. Determining how much arable land has been lost and the potential causes of arable land losses is crucial because agriculture is the basis of food security.

Previous studies show that the farmland area is on a decline. Studies also reveal that the total yield on the piece of land using the same techniques will decrease sooner than later due slow implementation of the high-standard farmland (Zhang & Yu, 2016). The study on the conflict between wild boars and farmers (Liu et al., 2019) indicated that farmland destruction has been more frequent and seriously observed in the

last 4–5 years, while farmer’s compensation was recommended. There has been no strict restriction on the construction of high-standard farmland on farmland ecology, and little attention has been paid to the environmental impact assessment (Yang et al., 2022). The construction of high-standard farmland has yielded positive results (Luoman et al., 2019). Mostly, the literature only shows the benefits of high-standard farmland construction. However, there are no studies on high-standard farmland destruction due to human activities.

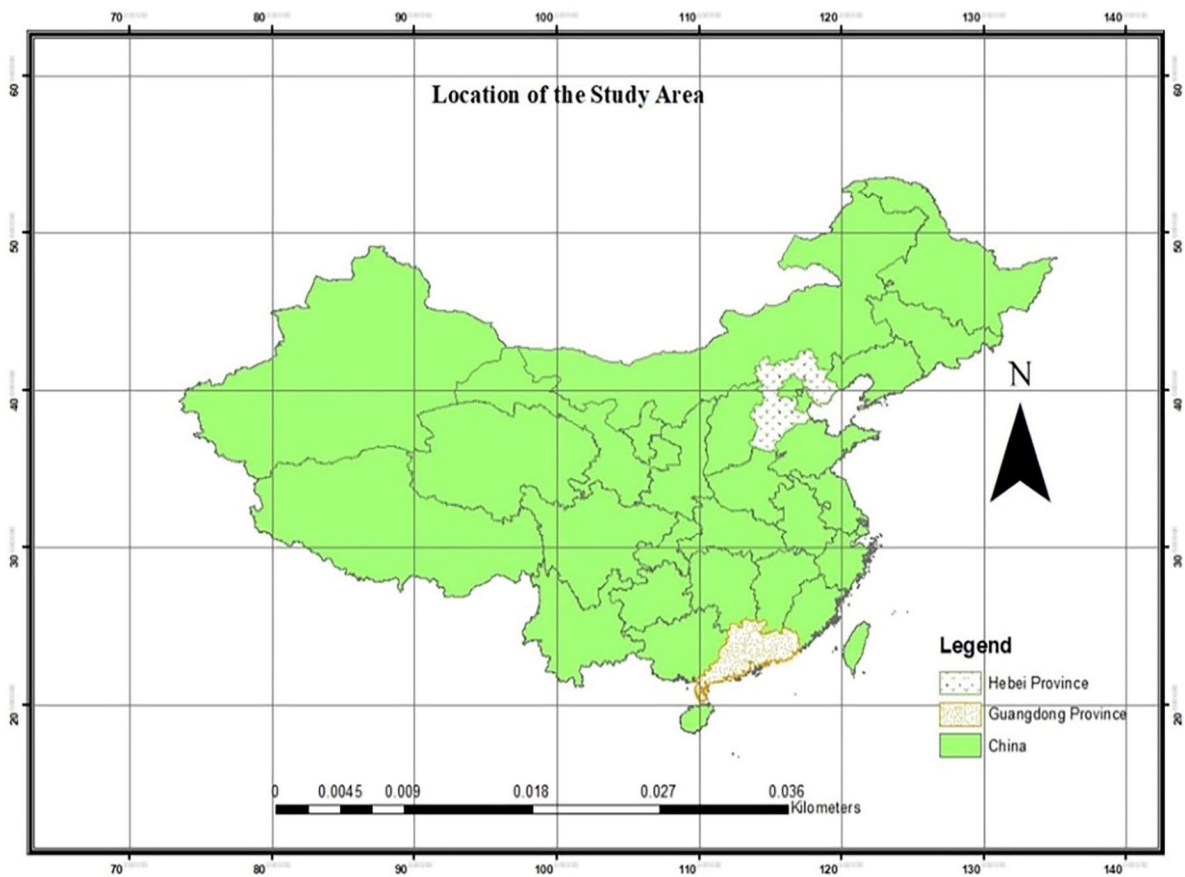
Therefore, this study demonstrates remote sensing monitoring techniques and methods to monitor the usage of high-standard farmland in China by processing Gao Fen-2 (GF-2) during 2017–2018 for Hebei and Guangdong provinces guided by the national guidelines of the high-standard farmland construction guidelines of 2011. The analysis targets high-standard farmland destructions on arable land by identifying

the causes, and the degree of destruction, by complying with a statistical summary of the violation in the study area.

### Research data and methods

#### Study area

This study was conducted in two provinces: (1) Hebei province in northern China was selected as the primary study location due to its usually continental climate, characterized by dry, cold winters and warm, rainy summers (Fig. 1). This region is influenced by cold air from neighboring Siberia during winter, while monsoons characterize the summer. The northeastern part of China is mostly dry, except in the summer. The area enjoys an average of 2700 h of sunshine annually, making it one of the sunniest places



**Fig. 1** Location of the study area

on Earth. The weather in the province is typical of the continent. January averages drop to  $-4\text{ }^{\circ}\text{C}$  in the south and  $-10\text{ }^{\circ}\text{C}$  in the north of the Great Wall. In the North China Plain, temperatures average around  $25\text{ }^{\circ}\text{C}$  in July, whereas in the northern and western highlands, they range from  $23$  to  $25\text{ }^{\circ}\text{C}$ . Most provinces receive yearly precipitation of over 20 inches (500 mm) of rain and snow. The rainy season occurs during the summer months of June, July, and August. The province of Hebei is an important agricultural center in China, producing grain and cotton. Wheat, corn (maize), kaoliang (a type of grain sorghum), millet, and potatoes are some of the most common cereal crops, and they may often be harvested in three cycles over 2 years. (2) As the southernmost province in China, Guangdong borders the South China Sea.

High temperatures and abundant rainfall are typical of the tropical and subtropical climates in the study area. In July, the average temperature is around  $28\text{ }^{\circ}\text{C}$ ; in January, it drops to approximately  $13\text{ }^{\circ}\text{C}$ . Precipitation averages between 1500 and 2000 mm per year. The months of July and August are prime typhoon seasons along the coast of Guangdong Province.

#### Data source and usage

Since Gaofen-2 is the first Chinese civil satellite with a resolution of more than 1 m, the study uses photos retrieved on 15 February 2017. It is a multi-purpose optical satellite with two pan-and-tilt-and-zoom (PAN/MSS) cameras covering 45 km simultaneously. 450–520 nm (blue), 520–590 nm (green), 630–690 nm (red), 770–890 nm (near-infrared), and a panchromatic band (450–900 nm), with a spatial resolution of 0.81 m, are all present in the Gaofen-2 imaging (Table 1). For forest cover monitoring, we use the overlap between five Gaofen-2 multi-spectral photos, with the mathematical basis playing a key role in defining a specific geographic region.

**Table 1** Gaofen-2 (GF-2) satellite image utilization

Satellite name	Date	Data type
GF2_PMS1_E113.7_N22.8_20170215_L1A0002187735	2017/02/15	MSS/PAN
GF2_PMS1_E113.7_N23.0_20170215_L1A0002187747	2017/02/15	MSS/PAN
GF2_PMS2_E113.8_N22.6_20170215_L1A0002187870	2017/02/15	MSS/PAN
GF2_PMS2_E113.9_N22.8_20170215_L1A0002187868	2017/02/15	MSS/PAN
GF2_PMS2_E113.9_N22.9_20170215_L1A0002187863	2017/02/15	MSS/PAN

#### Remote sensing data source selection methodology

GF-2 satellite characteristics listed in Table 2 clearly distinguish buildings, roads, pit ponds, farmland, and so on, while a pixel-based approach is required in other sensors. GF-2 satellite image easily identifies and distinguishes features, and the variation of information extracted by its accuracy is also higher. By comparing the resolution of the main products, the applicable band, width, price, and cost of data, combined with the requirements of the study image accuracy and the applicable band conditions, the GF-2 images were selected in order to ensure the accuracy of image classification and interpretation.

#### Image pre-processing procedures undertaken

##### *Radiometric calibration*

The radiometric calibration coefficient of the remote sensor is a quantitative transformation between digital number (DN) value and observed physical quantities. The top of atmosphere (TOA) reflectance of the earth's surface detected by the Gaofen-2 satellite was computed. Furthermore, in radiometric correction, radiation correction is mainly for remote sensing images to remove haze and thin clouds (Hoja et al., 2008). The removal of haze (thin clouds) is essential to correct the pixel value of the haze (thin cloud) area image using filtering to make it appear normal (Walter, 2005).

##### *Atmospheric correction*

The Envi 5.3 software was used for atmospheric correction for all five Gaofen-2 images used in the study. In contrast to previous atmospheric correction concepts, it uses only scene information (seen pixel spectra) to calculate atmospheric compensation

**Table 2** GF-2 satellite characteristics

Parameter	1 m full-color resolution/4 m resolution multi-spectral camera	
Spectral range	Panchromatic	0.45–0.90 μm
	Multispectral	0.45–0.52 μm
		0.52–0.59 μm
		0.63–0.69 μm
		0.77–0.89 μm
Parameter	1 m full-color resolution/4 m resolution multi-spectral camera	
Spatial resolution	Panchromatic	1 m
	Multi-spectral	4 m
Width	45 km (2 camera combination)	
Revisit the cycle (sideways)	5 days	
Cover cycle (non-side)	69 days	

parameters. The use of satellite imagery to make exact adjustments to geometry and radiometry is becoming crucial (Itten & Meyer, 1993).

*Geometric correction*

The Gaofen-2 satellite image collected on 2017/02/15 was subjected to geometrical modifications utilizing Ground Control Points (GCP) computed with a differential GPS Hossain et al., (2019). In this study, the results were set from cartographic map projection using Gaussian Kruger projection, 3 degrees zoning, a plane coordinate system using the 1980 Xi'an coordinate system, elevation system using the 1985 national elevation benchmark, and IUG1975 ellipsoid, which is a standard geodetic procedure for Chinese map. Ad hoc methods are summarized into two equations (Hoja et al., 2008). Spatial distortions are typically found in aerial and satellite photographs of land surfaces due to terrain relief and off-vertical imaging geometry. Some vertical ground features are distorted, meaning they were seen in a position where they are not in real-time. Geometric errors can be mitigated with the help of ancillary data, which includes instrument calibration information and details about the spacecraft's attitude, position, and velocity (Arif et al., 2006).

*Image mosaicking*

Finally, Image Mosaic should be conducted in order to achieve the purpose of strict splicing, the spliced

data can be uniformly arranged on the control points, and a polynomial correction method is adopted to correct the edge area of the image and control the error within 1 pixel. The process of merging images is critical when one has taken into consideration the spatial and spectral resolution. Most images might have a good resolution but not panchromatic and multi-spectral scenes. Therefore, the merging image process is applied to make the best of each image. Two images are overlaid together to produce a high-resolution image (Batini et al., 2017).

*Principal component transformation*

As the main component of transformation, principal component transformation (PCA) converts the highly correlated information in each band to a few components by rotating the remote sensing multi-spectral image data. As far as possible, to ensure that this component information is irrelevant (decorrelation), the multi-band original image is thus represented by a linear combined information image of several bands. Since the first few principal components of the principal component transform contain the main feature information and the noise is relatively small, it can highlight the main information and suppress the noise to achieve the image enhancement effect (Ma et al., 2017).

Choosing the best band principle

The bands involved in color synthesis must contain a large amount of information, giving the required and

desired output. The correlation between the bands involved in color synthesis is small, the color images synthesized by band combination must have large differences in spectral differences between the types of features of interest in the study area, the information content is significant, the correlation is small, there are spectral spectrum differences, and separable good band combination is the best combination. The best index method (OIF) proposed by the United States Chavez considers the information amount of the single-band image and the correlation between the bands. It is closer to the principle of band selection. The calculation is simple and easy to implement and has been widely applied. The formula is as follows:

$$OIF = \sum_{i=1}^3 Si / \sum_{j=1}^3 |R_{ij}| \quad (1)$$

Among them,  $S_i$  is the standard deviation of the  $I$  band, and  $R_{ij}$  is the correlation coefficient of two bands of  $i, j$ . In sorting the OIF index from big to small, in theory, the band combination corresponding to the largest OIF index is the best. Still, it must be judged according to the actual situation (Behairy & Khorsheed, 2007). Therefore, it should be judged according to the visual interpretation result. Firstly, each band was divided into groups according to the correlation analysis of each band of GF-2 data, and then the band combination according to the division result, as shown in Table 3.

Based on the correlation analysis of GF-2 data, we can see that the optimal index of 1 3 4 band combination is the best by calculating the best index of the 3 groups of bands and choosing these 3 bands' combination as the best band combination of information extraction, which can contain the largest amount of information. The boundaries between water bodies, vegetation, and buildings are clearly

visible on the GF-2 data using 3 4 1 band natural color composite images.

### Ground inspection

The process of ground verification is very critical for the assessment of classification results, remote sensing information extraction, field verification, and result compilation quality. The team corrected the existing problems in a self-test and mutual inspection and ensured the reliability and authenticity of the results. Ground truthing was conducted to prove the study's accuracy by going into the field with a Geographical Positioning System (GPS) device to locate and assess the targeted areas using a field sheet. A preliminary remote sensing interpretation is compiled, and a field investigation should be conducted to verify the initial translation results (Hu et al., 2010), an important procedure in RS science.

## Results

### Image interpretation and field investigation combined methods

#### *Human-computer interaction interpretation*

The information extraction method in this project was mainly man-machine interactive interpretation to ensure the accuracy of information extraction. Man-machine interactive interpretation is directly on the computer screen, with advanced remote sensing image processing software directly delineated, outlining the high standard of farmland boundaries (Blaschke, 2010). Image-based object identification

**Table 3** GF-2 (multi-spectral) correlation coefficient matrix table

Significance of bold entries is to put emphasis on the appropriate band combination required for the appropriate information extraction and analysis

Band	Band 1	Band 2	Band 3	Band 4
Band 1	1.000000	0.950818	0.904373	0.336042
Band 2	0.950818	1.000000	0.966929	0.430137
Band 3	0.904373	0.963929	1.000000	0.408729
Band 4	0.336042	0.430137	0.408729	1.000000
GF-2 data combination schemes and OIF values				
Band combination	<b>Band 1/2/4</b>	<b>Band 1/3/4</b>	<b>Band 2/3/4</b>	
OIF value	290.5204	366.1666	352.6001	

was generally approached in one of two ways. Firstly, region-growing techniques can be employed to adjacent group pixels with similar spectral values into individual objects (Aplin & Smith, 2008). The computer screen achieves information extraction which can be arbitrarily enlarged or reduced, accurately determining the location or recourse to the border (Zlinszky et al., 2017).

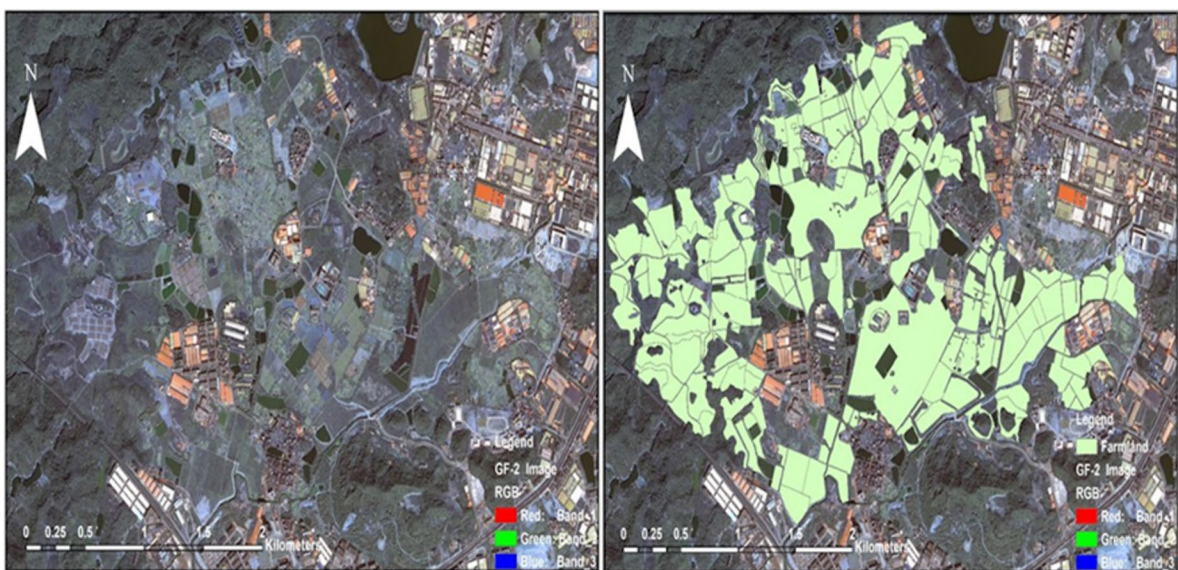
The “image object” is the primary theoretical unit of object-based image analysis, and it falls within the realm of inquiry midway between the technologically detectable and the practically plausible (Lang, 2008). The knowledge of the human expert who commands the computer to identify specific objects is key to determining the particular objects on the image (Blaschke et al., 2014). Combine the process of image segmentation with categorization based on prior experience. In addition, picture segmentation simplifies the substance of images by reducing the amount of detail present in them. Once evaluated and deemed significant, the picture sections formed by segmentation become image objects (Hossein et al., 2019; Hay & Castilla, 2006). It adopts the combination of route survey and point observation, where the key areas of the field survey are mainly the areas with a low level of interpretation and unclear spots and where only

remotely sensed imagery is available, and objects can be identified based on (spatial) patches of spectrally similar pixels (Aplin & Smith, 2008).

Following a segmentation approach, several authors (Piazza et al., 2016; Yan et al., 2006) have claimed that image segmentation is intuitively attractive and that human vision typically divides images into homogenous areas first and then characterizes those areas more carefully. Baoding County, Hebei province, in the North of China, was first processed and analyzed. Later, Dongguan County, Guangdong province, in South China, was interpreted using similar techniques (Fig. 2). By correctly segmenting an image into meaningful items of the land surface and land cover, it is suggested that more significant, logical, and intuitive outcomes would be achieved (Blaschke, 2000; Aplin & Smith, 2008).

Remote sensing images carry a broad amount of spatial information because they carry spatial information for larger geographical areas. Traditionally, remote sensing was used as a data-generating tool before the raster or vector GIS’s analytical capabilities were applied, making the transition from multi-spectral to thematic data a one-way route (Blaschke et al., 2000; Ruddick et al., 2005).

## High Standard Farmland Detection






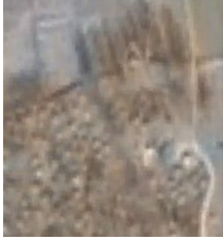
**Fig. 2** High-standard farmland detection

High-standard farmland was identified using a farmland vector shapefile as a layout for the detection (Fig. 2). Once the target had been identified, the classification process was conducted to delineate the study's area of interest. Upon completion of the interest area, the identification process of image features follows to determine the circumstances of the farmland in the interest area. Furthermore, suspicious and irregular features identified were recorded on a physical form for a statistical compilation to determine the extent of irregularities and features of interest detected during the investigation (Table 4).

According to Lizarazo (2014), the quality of the information that may be retrieved from remotely sensed data is determined mainly by the accuracy assessments performed.

The image feature must be properly identified and interpreted, and categorized into accurate homogeneity. The features identified during image analysis correctly classify the identified targets, among which was unutilized land, especially in Hebei province (Table 4). Land conversions were also detected, destructions to farmland were observed, and buildings on farmland were observed. Differences in texture, color, and shape directed the classification

**Table 4** Remote sensing interpretation of high-standard farmland construction and utilization monitoring

Suspected pattern type	Data type and timing	Area	Interpretation sign	Sample image
<b>Occupation of arable land</b>	GF-2 (2017.2.15)	Dongguan 113.987143 22.937671	The image shows dark green color, continuous dense, texture features obvious, and more uniform shades of color in the plain area showing occupation on arable land	
<b>Destruction of arable land</b>	GF-2 (2017.2.15)	Dongguan 113.650157 23.033214	The image was grey, a more uniform color, flaky, and continuous. The land has been destroyed and is no longer fertile for cultivation	
<b>Usage conversion of arable land</b>	GF-2 (2017.3.7)	Baoding 115.346923 38.895033	Image color and farmland have larger color differences, the outline of a clear regularity. Land use has been converted	
<b>Unutilize darable land</b>	GF-2 (2017.3.7)	Baoding 115.165049 38.619324	Differences in texture and farmland are large with shades, dark green spots scattered, no plate or stripline	



process, and suspected features were noted and then identified.

*Detected farmland destructions and field survey*

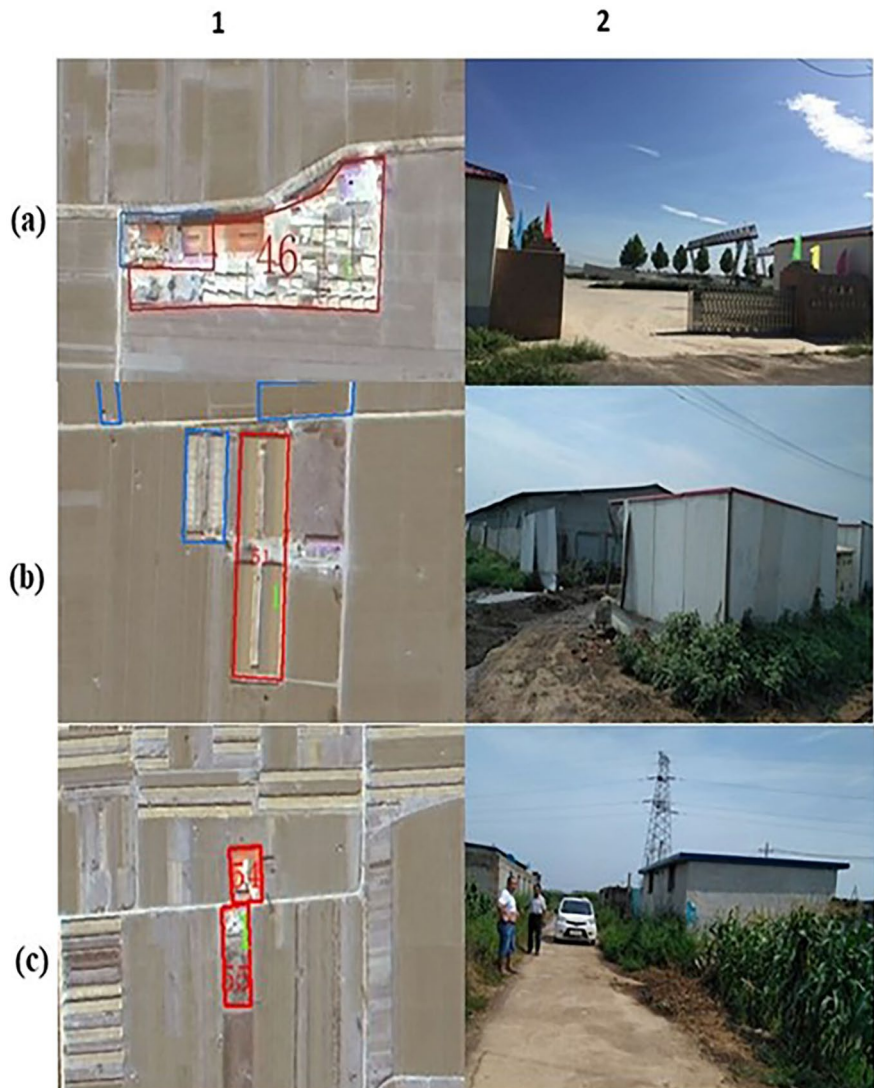
After the preliminary remote sensing interpretation is compiled, a field investigation should be conducted to verify the initial translation results (Hu et al., 2010). Field investigation and verification give a detailed survey and understanding of the high standards of farmland in the study area. They can be conducted on the whole to verify the reliability of the computer information extraction results and the plaques. It

helps the researcher to add missing information and modify inaccurate information.

Thus, farmland conversions were identified and verified in the Hebei province Baoding Area interpreted and ground verification images (Fig. 3).

**Field survey methods and requirements** Before the field verification work, formulate a field verification route based on the indoor interpretation situation, select the field verification points, and conduct field verification work on this basis. Field survey spot total requirements should equal the interpretation of the total number of suspected patches. The targeted areas and ground verification in Hebei province show

**Fig. 3** Farmland conversions identified and verified in Hebei province Baoding Area. (1) Interpreted image and (2) ground verification image. **a** Domestic compound. **b** Domestic shack. **c** Domestic factory



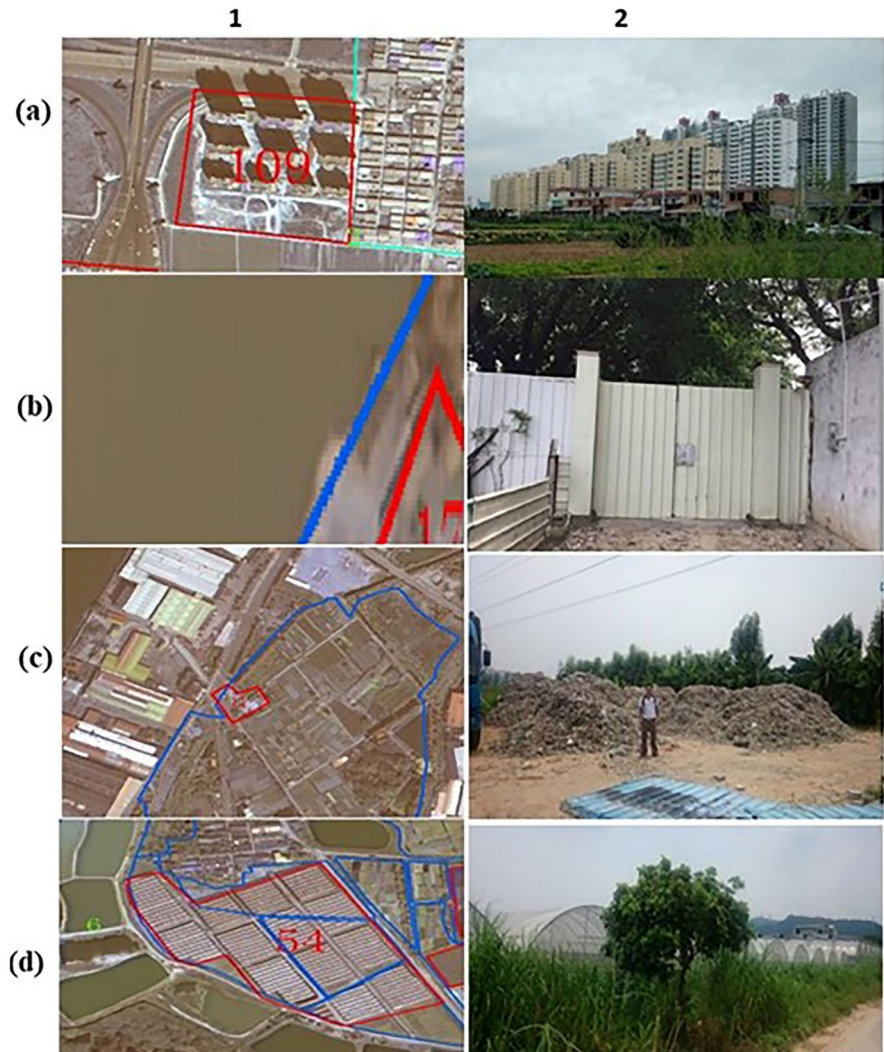
that illegal farmland occupation and identified and registered conversions were mainly due to domestic purposes. The presence of a domestic compound in the middle of the farmland shows that the local community's residential needs necessitated the conversion (Fig. 3a, b), and the occupation detected was informal residential shacks, chicken scoops, and domestic buildings, which were once again constructed on the farmland. Furthermore, the buildings identified were for domestic purposes and on a minimal scale (Fig. 3c). The damage observed was not extensive and did not pose a great environmental risk.

There is a different and contrasting phenomenon (Fig. 4) compared to Hebei province (Fig. 3),

where farmland detected was mostly domestically motivated.

The south of China in the targeted areas indicated that detections registered were rather commercial and on a larger scale. As shown in Fig. 4a, the farmland has been transformed into high-rise residential apartments which cover a large area of the farmland. The number of apartment blocks counted was 7 in total, as can also be observed in the image (Fig. 4b). The farmland has been turned factory, and high-rise walls were installed to block access. Farmland has been destroyed for sand mining, an indication of a boom in the construction industry, which has negative environmental implications in the long run (Fig. 4c). The farmland was still being utilized in Guangdong

**Fig. 4** Farmland conversions identified and verified in Guangdong province. (1) Interpreted image and (2) ground verification image. **a** Residential apartment. **b** Factory. **c** Sand mining. **d** Agricultural advancement



provinces (Fig. 4d), and very advanced methods were deployed to maximize the available remaining arable farmland. The build-up area encroaching on the farmland was one of the regular findings, as more build-up structures were discovered in the areas that were classified as high-standard farmland (Fig. 5).

In the figure, yellow represents the farmland build-up structures in the classified image, green represents high-standard farmland, and blue represents farmland irrigation, which has been reduced. The conversion of farmland into other economic activities such as residential apartment blocks, office complexes, industrial warehouses, and factories was observed.

The farmland land use and land cover classification map of the GF-2 image in Guangdong provinces is shown in Fig. 5b. The red color represents bare soil, blue for water, green for cultivated farmland, yellow for build-up areas, and black for roads. Arable farming land has been destroyed and is now used to supply sand for construction (Fig. 5b). Red shows that part of the farmland can no longer be used for cultivation due to the destruction, the topsoil has been removed, and the area is completely exposed.

A statistical compilation of farmland destruction

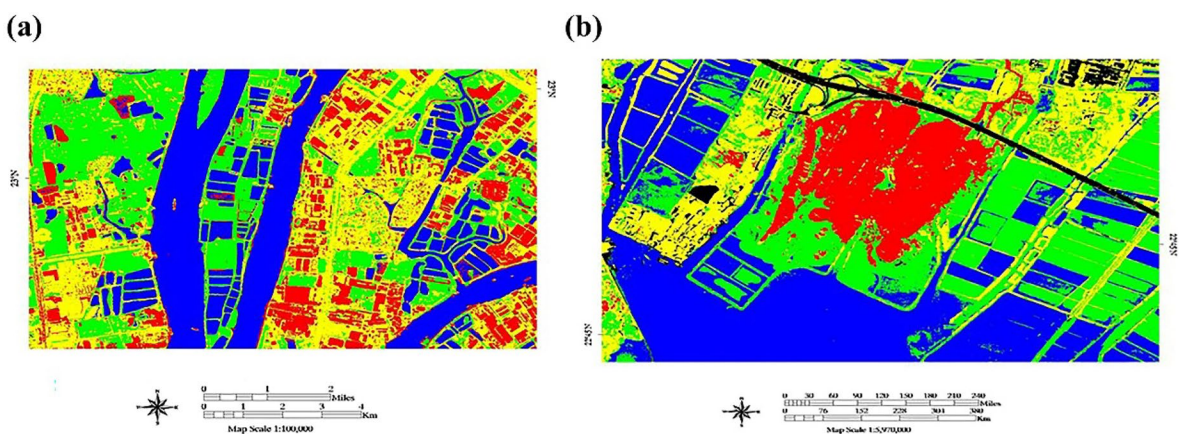
*Hebei province farmland destruction statistical summary*

North China’s economy is relatively traditional; therefore, the evidence shows that the destruction occurred due to domestic activities rather than commercial

purposes. Therefore, most of the arable land is still available and can be classified as high-standard farmland. In Mancheng County farmland construction projects, only 0.3464% of the total area of 45,876.53 M<sup>2</sup> has been taken up and transformed into residential shakes on the farm, and illegal activities destroyed about 0.7%. In Baoding New Urban Jiangcheng basic farmland finishing, only about 1.3889% was taken up from an area of 208,476.33 M<sup>2</sup>.

Many small towns in Hebei province showed little evidence of destruction. In Mancheng full town and the South Korean village, the basic farmland finishing project was destroyed from an area of 43,089.68 M<sup>2</sup>, and only 0.3072% was found not to meet the requirements, which is significantly low and not considered high risk. In Dingzhou City, Zao Zaozhen high village, and other (21) villages, the high-standard basic farmland construction soil was found to have the highest destruction in Hebei province at 13.2513% from an area measuring 6,475,338.35 M<sup>2</sup>. Many villages were moderate to low impact destruction, meaning most of the farms assessed complied with the regulations.

Object-based image analysis (OBIA) accuracy was considerably higher, particularly for the buildings, roads/railroad, and agriculture classes (MacFaden et al., 2012). This was attributed to the addition of high-quality thematic vector datasets for these characteristics. Outlining challenges, especially in Hebei province, satellite images showed evidence of destruction to farmland. However, the identified objects and features required ground visits to properly



**Fig. 5** **a** Build-up encroaching onto the farmland. **b** Map classification of farmland destruction

establish the current land use land cover change. Illegal farmland destructions were classified into four categories: taken up, destroyed, converted, and shortage. Table 5 gives a statistical compilation of how the north of China's high-standard farmland was detected from various villages and towns within the targeted study area.

#### *Guangdong province farmland destruction statistical summary*

The illegal establishment of high-standard farmland is derived from economic interests. Many people around the world in recent years have preferred to live in urban areas due to the economic benefits that come with especially people in the developing

world (PAI, 2011), and this has led to a decrease in available agricultural land, pushing most people to overcrowding conditions and illegal land occupation.

For example, in the more developed economy of Guangdong province, mostly illegal activities are driven by economic interests, and a higher percentage of land is fast transformed for economic activities like the construction of real estate on previously classified farmland. In Dalingshan Town, Dongguan City, of a 31,001.2869 M<sup>2</sup>, 2.3617% was destroyed, which is far less destruction in comparison to other towns in Guangdong provinces, Shenzhen Guangming Northland development, and consolidation of arable land project, where from an area of 237,841.9601 M<sup>2</sup>, 19.6281% was found to been destroyed which

**Table 5** Baoding high-standard farmland statistical usage summary results (unit: square meters)

Name	Area	Status	Problem area	Problem area %
Mancheng County 100,000 mu of high-standard basic farmland construction projects	64,942,737.93	Taken up	224,931.13	0.3464%
		Destroyed		
		Converted	28,964.02	0.0446%
		Shortage	45,876.53	0.0706%
Baoding New Urban Jiangcheng basic farmland finishing	15,010,404.35	Taken up	208,476.33	1.3889%
		Destroyed		
		Converted	5005.94	0.0333%
Mancheng full town, South Korea village basic farmland finishing project	14,025,787.40	Shortage	2879.27	0.0192%
		Taken up		
		Destroyed		
Dingzhou City, Zao Zaozhen, high village, and other (21) villages' high-standard basic farmland construction soil	48,865,681.15	Converted	43,089.68	0.3072%
		Shortage	43,089.68	0.3072%
		Taken up	6,475,338.35	13.2513%
		Destroyed		
Dingzhou City breeze shops and stay in the town of high standards of basic farmland construction land improvement project	25,337,988.80	Converted	28,208.73	0.0577%
		Shortage	28,208.73	0.0577%
		Taken up	1429.21	0.0056%
		Destroyed		
Baoding North District Han Zhuang Township, Hundred House Township, East Jin Zhuang basic farmland finishing	4,073,182.92	Converted	6781.70	0.1665%
		Shortage	6781.70	0.1665%
		Taken up		
		Destroyed		
Qing Yuan County, South Camp, Shao Zhuang village basic farmland finishing	4,736,968.87	Converted	483,440.34	11.8689%
		Shortage	483,440.34	11.8689%
		Taken up	85,401.1300	2.0967%
		Destroyed	85,401.1300	2.0967%
		Converted	71,777.05	1.5153%
		Shortage	71,777.05	1.5153%
		Taken up		
		Destroyed		
		Converted	3120.57	0.0659%
		Shortage	3120.57	0.0659%
		Taken up		
		Destroyed		

is quite a significant loss of arable land. However, in Shenzhen Guangming Northland development and consolidation of the arable land project (03-3b), from 38,785.3248 M<sup>2</sup>, there is 30.5946% loss of arable land, while in Shenzhen Guangming Northland development and consolidation of arable land project, from 15,559.5069 M<sup>2</sup>, 40.6603% of arable land was destroyed or transformed into residential properties. There is evidence of up to 40% loss of land in Shenzhen because the city has transformed from a rural agricultural economy to becoming the technological hub of China. Evidence from Table 5 is a statistical summary of farmland destruction in different selected towns and villages in Guangdong province.

### Arable land availability in China

By the early 1960s, 36.42% of the land had been converted into agricultural land, and China saw an increase in agricultural land due to friendly central government policies aimed at achieving food security for the country. The trend continued to rise steadily; in 1977, there was 43.86% already available. Rapid urbanization and the expanding needs of China’s industrial and agricultural economies have strained the country’s limited land resources. It can be observed that from the mid-90 s, China’s agricultural land expansion was slowing down (Fig. 6), and it had only increased by 1%, which at its highest record in

2009 was 56.13%. From 2009, it can be observed that land was being lost slowly. By 2020, only 56.06 of land could be classified as agricultural land in China. The central government will acknowledge this threat. In response, “red lines” have been established to prevent industrial development on farms and to preserve natural forests, wetlands, and endangered species habitats from human development.

As a result, different climatic conditions determine the soil type and topography. Precipitation and temperature (Fig. 7) determine the type of agricultural activities, such as the kinds of crops and methods that farmers cultivate. It is important to note that China is a large, vast country with contrasting climatic conditions. Wheat, barley, and other grains are the most widely grown crops in north China because of their arid continental environment. A temperate continental climate and a temperate monsoon climate predominate in the Hebei province area. The average summer temperature is 20 °C, while the winter temperature is below 0 °C. Temperature fluctuations mark four seasons. July is the wettest month, while January is the coldest month. There is not much precipitation throughout the year, and the seasonal distribution is unequal, with summer being the season with the most precipitation. In China, there are several different climate types. From the southeast to the northwest, the precipitation lessens. Southeast coastal cities often get around 2000 mm. In regions along the Huai River

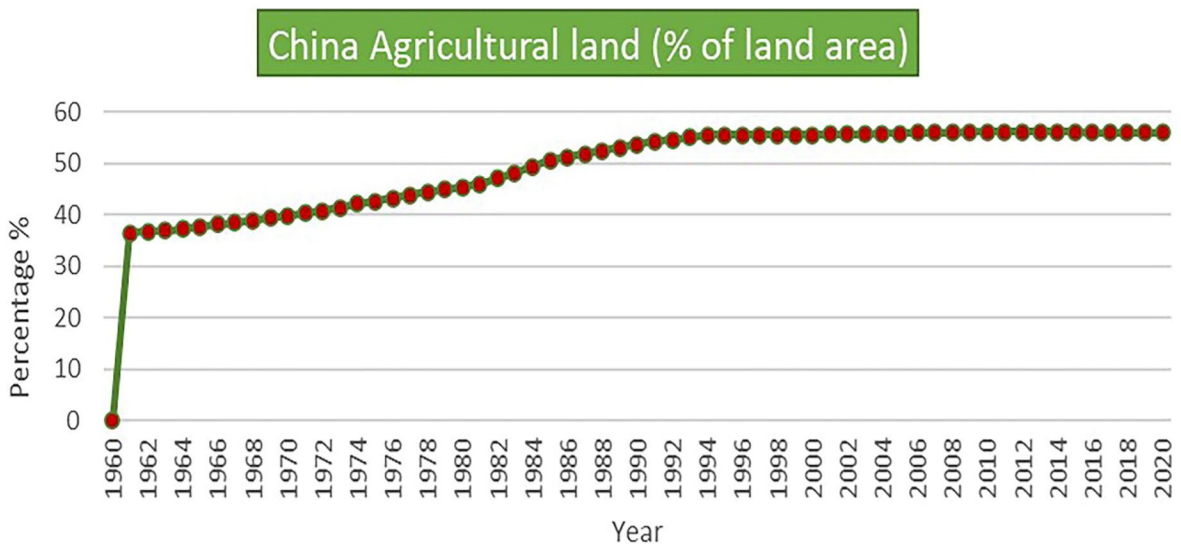
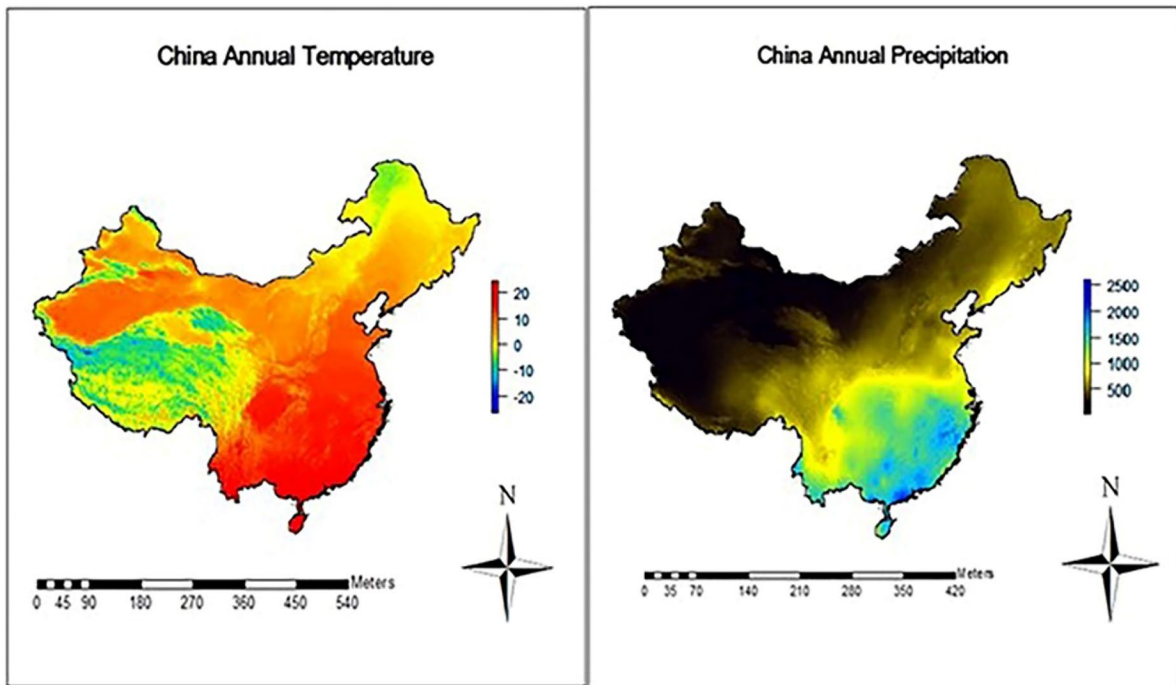


Fig. 6 China agricultural land area in percentage from 1960 to 2020



**Fig. 7** Annual temperature in China and annual precipitation map in China

further north, the annual rainfall drops to around 880 mm. Annual rainfall along the Yellow River's northeastern tributaries is about 600 mm. Typically, the rainy season begins in June and lasts until August. Therefore, summers are dryer, and winters are wetter. Understanding climate trends is crucial for high-standard farmlands to maintain high output.

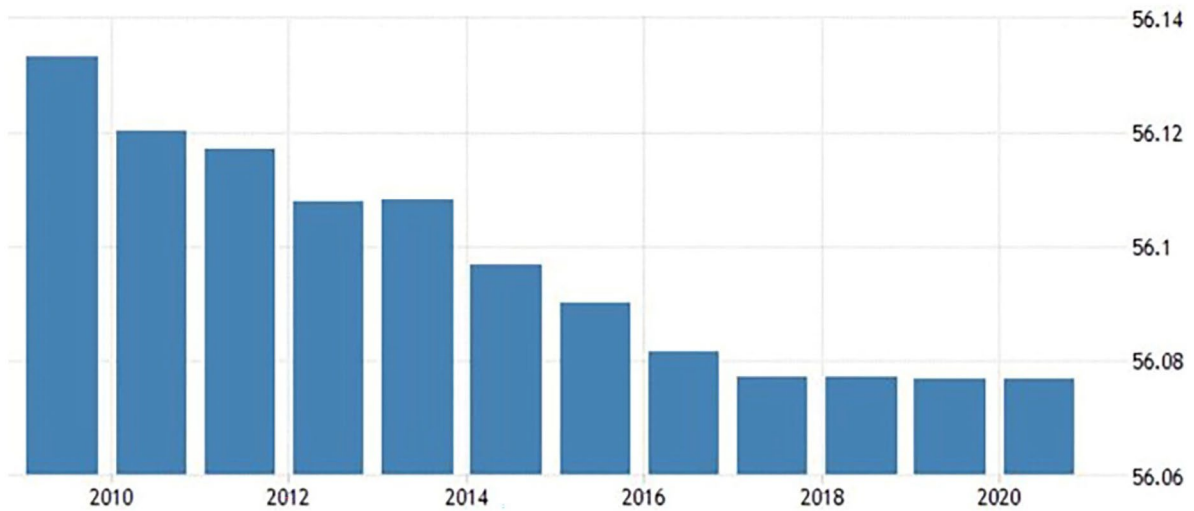
China's precipitation image shows that the southern provinces receive great precipitation. However, the results of this research show that the Guangdong province is losing more land due to rapid industrial development. China's temperature indicates the Guangdong province region is warmer compared to the northern region of Hebei, which indicates better favorable farming conditions in the south. However, the south is vulnerable to climatic-induced natural disasters to its location. China's arable land from 2010 to 2020 shows a steady decline (Fig. 8), exacerbated by industrialization.

The concerning trend reveals China's rapidly declining arable land availability (Fig. 8). In 10 years, the arable percentage has reduced from 56.13% in 2010 to 56.06% in 2020. There is a threat to high-standard farmland in China considering

the increase of industrialization in the Guangdong province regions for domestic purposes in the north. Regardless of the circumstances and the causes thereof, it is clearly evident that arable land is under threat which is significant for four reasons: high population pressure, industrialization, climate, and topography. As seen in Table 6, most land losses occur in Guangdong provinces, where farmland is converted into economic generation uses such as warehouses, residential blocks, and factories. The losses are caused by industrial expansion and demand.

Furthermore, arable land has been converted into other economic and domestic activities, which further puts pressure on the already scarce arable land resources, as shown in Figs. 3 and 4. Furthermore, a significant amount of arable land (Li et al., 2018) has been transferred to cooperatives seconded by firms and, thirdly, into other economic activities. However, what is significant is that agricultural land has been transferred into other sectors of the economy, which threatens the sustainability and availability of arable land.

In order to convert underutilized farmland, land with low productivity or property is classed as waste in rural



**Fig. 8** China arable land rapid decline over 10 years from 2010 to 2020 (Trading Economics, 2022)

areas. Farmers should be able to sell or lease their land to those with higher agricultural standards. Since the 1980s, the transfer of rural land has been legal, and it has since garnered the backing of the federal government. The Land Contract Law of China formalized the land transfer procedure in 2002. From 2007 to 2017, the percentage of arable land transferred increased dramatically, from 5 to 36.5% (Li et al., 2018).

**Discussion**

Hebei and Guangdong province’s contrasting circumstances

North China’s economy is relatively traditional, with most still traditional agriculture, with some farms qualified for the classification of high-standard farmland agriculture and a small presence of the traditional manufacturing sector. The evidence shows that the destruction occurred for domestic purposes rather than commercial purposes. Therefore, most of the arable land is still available and can be classified as high-standard farmland. In Mancheng County farmland construction projects, only 0.3464% of the total area of 45,876.53 M<sup>2</sup> has been taken and transformed into residential shakes

on the farm. The land was 0.7% destroyed by illegal activities. In Baoding, New Urban Jiangcheng basic farmland finishing, only about 1.3889% was taken up from an area of 208,476.33 M<sup>2</sup>.

The destruction shown in the small towns of Hebei province was smaller in percentages. In Mancheng full town, South Korea village basic farmland finishing project, from an area of 43,089.68 M<sup>2</sup>, only 0.3072% was found to be destroyed, which is significantly low and not considered high risk. Dingzhou City, Zao Zaozhen, and other (21) villages around the high-standard farmland were found to have the highest destruction in Hebei province at 13.2513% from an area measuring 6,475,338.35 M<sup>2</sup>. The destruction in Hebei province was derived from farmers engaged in other domestic activities rather than for commercial purposes. Part of the arable land was turned into shelters, small accommodation complexes, chicken coops, etc. The assessment indicated that the damage, as seen above in Table 5, was not extensive.

OBIA demonstrated better accuracy using high-quality theme vector datasets for elements, including buildings, roads/railroads, and farms (MacFaden et al., 2012). But in crowded residential districts with a complex mosaic of grass lawns and concrete surfaces, several elements, especially those with closely similar spectral signatures, produced confusion

**Table 6** Dongguan area high-standard farmland usage statistical results (unit: square meters)

Summary	Area	Status	Problem map area	Problem area ratio
Dalingshan Town, Dongguan City, 2012 high-standard basic farmland construction projects	1,312,668.6757	Taken up		
		Destroyed		
		Converted		
		Shortage	31,001.2869	2.3617%
Dongguan Dao Zhen 2012 high-standard basic farmland construction projects	1,502,003.3790	Taken up	41,137.6656	2.7389%
		Destroyed		
		Converted	15,686.7426	1.0444%
		Shortage		
Shenzhen Guangming North land development and consolidation of the arable land project (03–2, 03–7)	1,211,744.0877	Taken up		
		Destroyed	7172.3728	0.5919%
		Converted		
		Shortage	237,841.9601	19.6281%
Shenzhen Guangming North land development and consolidation of the arable land project (03–11)	38,267.1159	Taken up		
		Destroyed		
		Converted		
		Shortage	15,559.5069	40.6603%
Shenzhen Guangming North land development and finishing supplementary farmland project second phase	254,356.1829	Taken up		
		Destroyed		
		Converted		
		Shortage	3833.1275	1.5070%
Shenzhen Guangming North land development and consolidation of supplementary farmland project (03–5, 8)	342,331.6370	Taken up		
		Destroyed		
		Converted		
		Shortage	26,441.6698	7.7240%
Shenzhen Guangming North land development and consolidation of the arable land project (03-3b)	126,771.5926	Taken up		
		Destroyed		
		Converted		
		Shortage	38,785.3248	30.5946%
Shenzhen Guangming North basic farmland improvement project (03–9)	40,695.0706	Taken up		
		Destroyed		
		Converted		
		Shortage		
Shenzhen Guangming North land development and consolidation of supplementary farmland project (03-3c, 4)	346,375.5651	Taken up		
		Destroyed		
		Converted		
		Shortage		
Shenzhen Guangming North land development and consolidation of arable land projects (03-3a)	705,654.5862	Taken up		
		Destroyed		
		Converted		
		Shortage	71,205.4286	10.0907%
Changping Town, Dongguan City, 2012 high-standard basic farmland construction projects	2,171,211.7689	Taken up	7410.4357	0.3413%
		Destroyed	3395.2241	0.1564%
		Converted	14,113.6866	0.6500%
		Shortage	146,159.6922	6.7317%



**Table 6** (continued)

Summary	Area	Status	Problem map area	Problem area ratio
Dongguan Dongkeng 2012 high-standard basic farmland construction project	690,920.9237	Taken up	3279.3598	0.4746%
		Destroyed	5009.1106	0.7250%
		Converted		
Shatian Town, Dongguan City, 2012 high-standard basic farmland construction projects	1,307,123.3494	Shortage		
		Taken up	35,088.3795	2.6844%
		Destroyed		
		Converted		
		Shortage		

between the grass and shrub classifications and other paved surface classifications, despite the general accuracy remaining higher. Outlining some of the challenges in the study, especially in Hebei province, satellite images showed evidence of destruction to farmland. However, the identified objects and features required ground visits to properly establish the current land use land cover change (Vasco, 2008; Hu et al., 2010; Piazza et al., 2016).

Land cover and land use question in China needs continuous follow-ups and monitoring, and spatial maps must be continuously monitored and updated. There is continuous and consistent loss of high-standard farmland for either industrial purposes in the south or farmland destruction by introducing other activities, such as sand mining, to cater to the greater boom caused by the estate development (Table 6). Similar work has already been conducted in the UK to update the object-based land cover map, with an additional recommendation to adapt digital cartography to give an object structure that more properly reflects the actual structure of the landscape (Aplin & Smith, 2008).

High-resolution GF-2 satellite images revealed a pattern of destruction to high-standard farmland in Guangdong provinces. Evidence shows that many farmers did not follow the national standard of farmland procedures as stipulated by the Ministry of Lands and Resources. There was an occurrence of illegal occupation and intrusion onto the farmland, which caused serious changes in land cover and land use through serious adjustments and desolation. Most farmland area has been transformed into farm parking, landfills, farm homes, and so on. Though the enclosing walls surrounding some farms made

it difficult to access some target areas located inside the farm, even with this obstacle, pictures were taken by climbing the wall and pointing the camera in the direction of the target.

The Guangdong province, especially in Shenzhen, has seen a boom in high-rise commercial and residential buildings in former farmland areas. Economic interests seem to be the driving factor leading to most violations in South China. However, in Dalingshan Town, Dongguan City, of a 31,001.2869 M<sup>2</sup>, 2.3% was destroyed, which is far less destructive than other towns in Guangdong provinces, which implies that most violations appear in the south of China. Smaller towns were less affected than bigger cities like Shenzhen. In Guangming Northland, development and consolidation of arable land project, from an area of 237,841.9601 M<sup>2</sup>, 19.6281% was found to be destroyed, which is quite a significant loss of arable land.

Furthermore, in the Shenzhen Guangming Northland development and consolidation of the arable land project (03-3b), from a total of 38,785.3248 M<sup>2</sup>, 30.59% of arable land was lost. Additionally, in Shenzhen Guangming Northland, the development and consolidation of an arable land project, of 15,559.5069 M<sup>2</sup>, 40.6603% of arable land was destroyed or transformed into residential properties, which is a significant loss. With these trends in the Southern city of Shenzhen, the problem of lack of arable land is being exacerbated at a very serious pace, which, if it is not controlled, will lead to an emergency crisis, if it is already not.

Furthermore, environmental damage can be observed in some high-standard farmland where sand mining and digging were taken because sand mining destabilizes soil structure. Because the top layer

of the soil is removed, the soil structure is affected. Operation of heavy equipment on the farmland directly destroys reproducing habitat fauna and flora habitat species. It is also not good, especially near the river, as it produces increased turbidity and suspended sediment downstream. Sand mining disturbs and completely removes the habitat from the mined zones. Noise is an issue in the mining areas because mine operations are 24 h a day. The noises pollute the environment and disturb people and the environment too. Once the sand is removed, it cannot be replaced as it is used elsewhere, e.g., in the construction industry. The environmental damage will stand for generations (Pitchaiah, 2017).

#### Implications of high-standard farmland destruction on food security

Rural households in China are increasingly obtaining their income from off-farm activities (OECD, 2018). As a result, it has already become a major source of income. This has led to the abandonment of farming activities. The extra income obtained from off-farming activities has motivated farmers to take more and more farming land into their off-farming activities, which are more profitable, which led to the abandonment of farming, as well as it has led to a reduction in the amount of agricultural land. It also noted that rising environmental concerns had become critical barriers to achieving sustained growth in agricultural output in China (OECD, 2018). The destruction of farmland due to sand mining, construction sites, factory warehouses, etc. has made future production trends questionable due to soil and water resource contamination and pollution. A policy approach to reducing and eventually reversing the existing practice of destroying farmland and chemical inputs and ameliorating these environmental limits where natural resources are being exploited is necessary for the sustainable productivity increase of agriculture. Advances can be important stepping stones to a more sustainable food system, although farmers who adopt them typically rely on high-risk or limited resources (Gliessman, 2014).

China has experienced a decline in the amount of cultivated land and a high proportion of smallholder farms. China's urbanization rate has been increasing since the introduction of the reform and opening-up policy in 1978, and cultivated land has been the primary source of building land growth, leading to the shrinking of

cultivated land, which was notably noticeable throughout the 1990s and 2010s (Wang et al., 2022).

Furthermore, land and water are both limited resources essential to agricultural development in China. Between 1991 and 2014, the extent of arable land fell by 15.3% (19.2 million hectares) due to increased competition from urban land usage. In 2015, urban or industrial land use comprised 4% of all land use, while agricultural land use comprised 40% (OECD, 2018).

Researchers discovered that socioeconomic and demographic characteristics, such as age, education, farming experience, and farm size, were all significant predictors of farmers' level of knowledge (Alotaibi et al., 2020). Therefore, all these factors are to be considered when implementing monitoring procedures. Population pressure burdens land use, and in China, there is an ever-increasing demand for farmers to produce more (Reis (2008). Therefore, the current trend of shrinking agricultural land is a serious concern for food security.

It indicated that most destructions were due to economic motivations. Farmers see that other industries are profitable and ready to abandon farmland for profitable economic activities (World Bank, 2007). To maintain a minimum of 307 million arable acres (named the "redline") by 2020, the Chinese government regularly monitors the net amount of arable land transferred to other activities to achieve food security.

The more farmers abandon the rural lifestyle for urban opportunities, and the more farmland is unsustainably mismanaged, the greater the risk of declining agricultural yield output. As the industry expands, agricultural land shrinks, and demand for food rises; this phenomenon, if not addressed, will exacerbate the crisis if it has not already, with implications on food scarcity, low yields, and high food prices due to rising imports. The Chinese central government has increasingly turned to rural construction land, which can be converted into arable land, of course, with compensation to the land owners (Xu et al., 2022). The findings from this study reveal that though policy efforts have been made, China continues to lose more land, which is a real threat to food security.

#### Conclusion

High-resolution GF-2 satellite images revealed a pattern of destruction to high-standard farmland in

Guangdong provinces. Evidence shows that many farmers did not follow the national standard of farmland procedures. Illegal occupation and intrusion onto the farmland caused serious changes in land cover and land use through serious adjustments and desolation. Most farmland area has been transformed into farm parking, landfills, and farm homes. The study further revealed that in Hebei province in northern China, farmland recorded destruction was mostly on a domestic scale. The observed destructions were for domestic farm homes, small-scale factories, the building of chicken scoops, landfills, and so on. It is important to note that there was less environmental destruction observed. Furthermore, Hebei province shows potential for greater high-standard farmland construction project expansion.

On the contrary, South China has lost so much land due to increased expansion and growing economic activities. The destruction and transformation of high-standard farmland are derived from economic interests. The high-tech industry, property development, and real estate have a boom in the south, which has led to higher violations of high-standard farmland construction guidelines as more farmland has either been converted for or destroyed by rapid industrialization. The environmental risk was higher due to arable land's unsustainable utilization and destruction. Finally, China faces a decline in arable land as farmers abandon agricultural activities for more high-income-generating projects. The rural population has dwindled, reducing agriculture employment to only 24%. Therefore, the state policy formulation and monitoring should continually evolve to the needs of the ground for China to save its arable land.

The more farmers abandon the rural lifestyle for urban opportunities, and the more farmland is unsustainably mismanaged, the greater the risk of declining agricultural yield output. As the other economic industries expand, agricultural land shrinks, and demand for food rises. If not addressed, this phenomenon will exacerbate the farmland scarcity crisis, if not already, which will have serious implications for food scarcity, low crop yields, and high food prices due to rising imports.

A 90% accuracy rate achieved by the study highlights the significant advantage of high-resolution remote sensing over traditional monitoring methods. Still, traditional methods should not be completely overlooked as, in some instances, a combination of

both methods can provide the best results. The long-term viability of the Chinese agricultural sector is greatly hampered by the country's enormous population and inadequate natural resources.

**Author contribution** Admire Muchimamui Mutelo: data collection, analysis, writing, investigation, methodology, writing—original draft, writing—review and editing, validation, and visualization. Chen Zhen: conceptualization, data collection, formal analysis, supervision and resources, data acquisition, validation, and visualization. Shen Wei: project administration, resources, software, supervision, validation, and visualization. Shindume Lomboleni Hamukwaya: research analysis, submission preparation, writing—review and editing, validation, and visualization. All authors reviewed the results and approved the final version of the manuscript.

**Data availability** The datasets generated during the current study are available from the corresponding author upon reasonable request.

#### Declarations

**Competing interests** The authors declare no competing interests.

#### References

- Alotaibi, B. A., Kassem, H. S., AL-Zaidi, A., & Alyafsi, A. (2020). Farmer's awareness of agri-environmental legislation in Saudi Arabia. *Land Use Policy*, 99, 104902. <https://doi.org/10.1016/j.landusepol.2020.104902>
- Alvarez-Vanhard, E., Corpetti, T., & Houet, T. (2021). UAV & satellite synergies for optical remote sensing applications: A literature review. *Science of Remote Sensing*, 3, 100019. <https://doi.org/10.1016/j.srs.2021.100019>
- Aplin P., Smith, G. M. (2008). Advances in object-based image classification, The International Archives of the Photogrammetry, *Remote Sensing and Spatial Information Sciences*, 37(B7), 725–728.
- Arif, M., Chohan, M. A., Ali, S., Gul, R., & Khan, S. (2006). Response of wheat to foliar application of nutrients. *American Journal of Agricultural and Biological Science*, 1(4), 30–34.
- Batini, C., Blaschke T., Lang S. Albrecht F, Abdulmutalib H M, Barsi S. G, Kugler Z. (2017). Data quality in remote sensing. International Archives of the Photogrammetry. *Remote Sensing and Spatial Information Sciences, ISPRS Archives*, 42(2W7), 447–453. International Society for Photogrammetry and Remote Sensing. <https://doi.org/10.5194/isprs-archives-XLII-2-W7-447-2017>
- Bahairy, H. M., Khorsheed M. S. (2007). Improving image quality in remote sensing satellites using channel coding. *International Journal of Computer and Information Engineering*, 1(9), 2888–2893. <https://doi.org/10.5281/zenodo.1330337>
- Bitelli, D., Conte P, De Giglio M, et al. (2017). Remote sensing for environmental monitoring, energy efficiency, and disaster management. *Geomatics-Remote Sensing*: 1–12.

- Blaschke, T. (2010). Object based image analysis for remote sensing. *ISPRS Journal of Photogrammetry and Remote Sensing*, 65, 2–16. <https://doi.org/10.1016/j.isprsjprs.2009.06.004>
- Blaschke, T., Geoffrey, H. J., Kelly, M., Lang, S., Hofmann, P., Addink, E., Raul, Q. L., van der Meer, F., van der Werff, H., van Coillie, F., & Tiede, D. (2014). Geographic object-based image analysis – Towards a new paradigm. *ISPRS Journal of Photogrammetry and Remote Sensing*, 87, 180–191. <https://doi.org/10.1016/j.isprsjprs.2013.09.014>
- Blaschke, T., Lang S., Lorup E., Strobl J., Zeil P. (2000). Object-oriented image processing in an integrated GIS/remote sensing environment and perspectives for environmental applications, *Environmental information for planning, politics and the public*, (2), 555–570.
- Ghuri, B., Zaidi A. (2011). Application of remote sensing in environmental studies. Department of Remote Sensing and Geo-Information Science, *Institute of Space Technology, Karachi Campus*, 1–8.
- Gliessman, S. R. (2014). *Agroecology: The ecology of sustainable food systems*, Third Edition (3rd ed.). CRC Press. <https://doi.org/10.1201/b17881>
- Hay, G. J., Castilla G. (2006). Object-based image analysis: Strengths, weaknesses, opportunities, and threats (SWOT). *The International Archives of the Photogrammetry, Remote Sensing and Spatial Information Sciences*.
- Hoja, D., Schneider, M., Lehner, M., & Reinartz, P. (2008). Comparison of orthorectification methods suitable for rapid mapping using direct georeferencing and RPC for optical satellite data. *International Society for Photogrammetry and Remote Sensing*, B4, 1617–1624.
- Hossain, M. A., Zahid, A. M., Arifunnahar, M., & Siddique, M. N. A. (2019). Effect of brick kiln on arable land degradation, environmental pollution and consequences on livelihood of Bangladesh. *Journal of Science, Technology and Environment Informatics*, 06(02), 474–488. <https://doi.org/10.18801/jsteei.060219.50>
- Hu, T. G., Zhu, W. Q., Yang, X. Q., Pan, Y. Z., & Zhang, J. S. (2010). Farmland parcel extraction based on high resolution remote sensing image. *Guang Pu Xue Yu Guang Pu Fen Xi*, 29(10), 2703–7. Chinese.
- Itten, K. I., & Meyer, P. (1993). Geometric and radiometric correction of TM data of mountainous forested areas. *IEEE Transactions on Geoscience and Remote Sensing*, 31(4), 764–770. <https://doi.org/10.1109/36.239898>
- Karthikeyan, L., Chawla, I., Mishra, A., & K. (2020). A review of remote sensing applications in agriculture for food security: Crop growth and yield, irrigation, and crop losses. *Journal of Hydrology*, 586, 124905. <https://doi.org/10.1016/j.jhydrol.2020.124905>
- Lang, S. (2008). Object-based image analysis for remote sensing applications: Modeling reality – Dealing with complexity. In T. Blaschke, S. Lang, & G. J. Hay (Eds.), *Object-based image analysis. Lecture Notes in Geoinformation and Cartography*. Springer, Berlin, Heidelberg.
- Li, C., Hayes, D., Jacobs, K. (2018). The “stover availability versus supply” puzzle and contracting options for cellulosic biomass. *Agricultural Policy Review*, Iowa State University. Retrieved from [https://www.card.iastate.edu/ag\\_policy\\_reviewon12/12/2022](https://www.card.iastate.edu/ag_policy_reviewon12/12/2022).
- Liu, Q., Yan, K., Lu, Y. F., Li, M., & Yan, Y. (2019). Conflict between wild boars (*Sus scrofa*) and farmers: Distribution, impacts, and suggestions for management of wild boars in the Three Gorges Reservoir Area. *Journal of Mountain Science*, 16(10), 2404–2416. <https://doi.org/10.1007/s11629-019-5453-4>
- Lizarazo, I. (2014). Accuracy assessment of object-based image classification: Another STEP. *International Journal of Remote Sensing*, 35(16), 6135–6156. <https://doi.org/10.1080/01431161.2014.943328>
- Luoman, P., Shuwen, Z., Jiuchun, Y., Fengqin, Y., & Liping, C. (2019). Assessment of high-standard farmland construction effectiveness in Liaoning province during 2011–2015. *Chinese Geographical Science*, 29(4), 667–678. <https://doi.org/10.1007/s11769-019-1061-z>
- Ma, L., Li, M., Ma, X., Ma, X., Cheng, L., Du, P., Liu, Y. (2017). A review of supervised object-based land-cover image classification. *Isprs Journal of Photogrammetry & Remote Sensing*, 130. <https://doi.org/10.1016/j.isprsjprs.2017.06.001>
- MacFaden, S. W., O’Neil-Dunne, J. P. M., Royar, A. R., Lu, J. W. T., Rundle, A. G. (2012). High-resolution tree canopy mapping for New York City using LIDAR and object-based image analysis. *Journal of Applied Remote Sensing*, 6(1), 063567. <https://doi.org/10.1117/1.JRS.6.063567>
- OECD. (2018). Innovation, agricultural productivity and sustainability in China. *OECD Food and Agricultural Reviews*, OECD Publishing, Paris. <https://doi.org/10.1787/9789264085299-en>
- Piazza, G. A., Vibrans, A. C., Liesenberg, V. R., Cesar, J. (2016). Object-oriented and pixel-based classification approaches to classify tropical successional stages using airborne high-spatial resolution images. *GIScience & Remote Sensing*, 1–21. <https://doi.org/10.1080/15481603.2015.1130589>
- Pitchaiah, P. S. (2017). Impacts of sand mining on environment – A review. *International Journal of Geoinformatics and Geological Science*, 4(1), 1–6. <https://doi.org/10.14445/23939206/IJGGS-V4I1P101>
- Population Action International (PAI). (2011). *Why population matters to food security*. Washington DC. Population Action International, 1–4. <https://toolkits.knowledgesaccess.org/toolkits/phe/why-population-matters-food-security>. Accessed 12 Dec 2022.
- Reis, S. (2008). Analyzing land use/land cover changes using remote sensing and GIS in Rize. *North-East Turkey. Sensors*, 8(10), 6188–6202. <https://doi.org/10.3390/s8106188>
- Roy, P. S., Behera, M. D., & Srivastav, S. K. (2017). Satellite remote sensing: Sensors, applications and techniques. *Proc. Nat. Aca. Sci., India. Sect. A Phys. Sci.*, 87, 465–472. <https://doi.org/10.1007/s40010-017-0428-8>
- Ruddick, K., De Cauwer, V., Van Mol, D. (2005). Use of the near infrared similarity reflectance spectrum for the quality control of remote sensing data, *Remote Sensing of the Coastal Oceanic Environment. International Society for Optics and Photonics*, 5885, 588501–588512. <https://doi.org/10.1117/12.615152>
- Trading Economics. (2022) *China arable land*. <https://tradingeconomics.com/china/arable-land-percent-of-land-area-wb-data.html> (retrieved 12/12/2022)

- Vasco, A. (2008). Remote sensing multi-spectral imagery processing in farmland inventory. *Journal of Information Control and Management Systems*, 11, 43–50.
- Walter, V. (2005). Object-based classification of integrated multispectral and LIDAR data for change detection and quality control in urban areas. In *the Proceedings of the ISPRS Joint Conference 3rd International Symposium Remote Sensing and Data Fusion Over Urban Area and 5th International Symposium on Remote Sensing of Urban Areas*, 14–16. Retrieved from <http://citeseerx.ist.psu.edu/viewdoc/summary?doi=10.1.1.61.755>
- Wang, D., Yang, H., Hu, Y., Zhu, A. X., & Mao, X. (2022). Analyzing spatio-temporal characteristics of cultivated land fragmentation and their influencing factors in a rapidly developing region: A case study in Guangdong province. *China. Land*, 11, 1750. <https://doi.org/10.3390/land11101750>
- World Bank. (2007). *World Development Report 2008: Agriculture for development*. Washington, DC. <https://openknowledge.worldbank.org/handle/10986/5990>, <http://hdl.handle.net/10986/5990>. Accessed 12 Dec 2022.
- Xu, R., Zhan, Y., Zhang, J., He, Q., Zhang, K., Xu, D., Qi, Y., & Deng, X. (2022). Does construction of high-standard farmland improve recycle behavior of agricultural film? Evidence from Sichuan. *China. Agriculture*, 2022(12), 1632. <https://doi.org/10.3390/agriculture12101632>
- Yan, G., Mas, J. F., Maathuis, B. H. P., Xiangmin, Z., & Van Dijk, P. M. (2006). Comparison of pixel-based and object-oriented image classification approaches—A case study in a coal fire area, Wuda, Inner Mongolia. *China. International Journal of Remote Sensing*, 27(18), 4039–4055. <https://doi.org/10.1080/01431160600702632>
- Yan, W. Y., Mahendrarajah, P., Shaker, A., Faisal, K., Luong, R., & Al-Ahmad, M. (2014). Analysis of multi-temporal Landsat satellite images for monitoring land surface temperature of municipal solid waste disposal sites. *Environmental Monitoring and Assessment*, 186(12), 8161–8173. <https://doi.org/10.1007/s10661-014-3995-z>
- Yang, X., Zhou, X., Shang, G., & Zhang, A. (2022). An evaluation on farmland ecological service in Jiangnan Plain, China-From farmers' heterogeneous preference perspective. *Ecological Indicators*, 136, 108. <https://doi.org/10.1016/j.ecolind.2022.108665>
- Zlinszky, A., Boergens, E., Glira, P., & Pfeifer, N. (2017). Airborne laser scanning for calibration and validation of inshore satellite altimetry: A proof of concept. *Remote Sensing of Environment*. <https://doi.org/10.1016/j.rse.2017.04.027>

**Publisher's note** Springer Nature remains neutral with regard to jurisdictional claims in published maps and institutional affiliations.

Springer Nature or its licensor (e.g. a society or other partner) holds exclusive rights to this article under a publishing agreement with the author(s) or other rightsholder(s); author self-archiving of the accepted manuscript version of this article is solely governed by the terms of such publishing agreement and applicable law.